



HAL
open science

Sensitivity analysis of human motion for the automatic improvement of gestures

Pauline Maurice, Vincent Padois, Yvan Measson, Philippe Bidaud

► **To cite this version:**

Pauline Maurice, Vincent Padois, Yvan Measson, Philippe Bidaud. Sensitivity analysis of human motion for the automatic improvement of gestures. 2015. hal-01221647v1

HAL Id: hal-01221647

<https://hal.science/hal-01221647v1>

Preprint submitted on 28 Oct 2015 (v1), last revised 6 Feb 2019 (v3)

HAL is a multi-disciplinary open access archive for the deposit and dissemination of scientific research documents, whether they are published or not. The documents may come from teaching and research institutions in France or abroad, or from public or private research centers.

L'archive ouverte pluridisciplinaire **HAL**, est destinée au dépôt et à la diffusion de documents scientifiques de niveau recherche, publiés ou non, émanant des établissements d'enseignement et de recherche français ou étrangers, des laboratoires publics ou privés.

Sensitivity analysis of human motion for the automatic improvement of gestures

Pauline Maurice, Vincent Padois *Member IEEE*, Yvan Measson, and Philippe Bidaud *Member IEEE*,

Abstract—Enhancing the performances of technical gestures is a great concern for human beings, and aims both at improving the operational results and at reducing the associated biomechanical demands. Thanks to the advances in human biomechanics and modeling tools, human performances can be evaluated with more and more details. However, finding the right modifications which improve such performances is still addressed with extensive time-consuming trial and error processes. This paper presents a method for automatically providing recommendations to improve human gestures. An optimization-based whole-body controller is used to dynamically replay human gestures from motion capture data, in order to acquire and evaluate the initial gesture. Virtual human simulations are then run to estimate performance indicators, when the gesture is performed in many different ways, in order to compute sensitivity indices for quantifying the influence of the gesture parameters on the performances. Based on this sensitivity analysis, recommendations for gesture improvement are provided. The whole method is validated on a drilling gesture. The consistency of the replayed motion and the significant increase in the performances of the gesture modified according to the provided recommendations confirm the relevance of the proposed approach.

Index Terms—Sensitivity analysis, Motion capture, Motion replay, Virtual human simulation, Whole-body control, Motion analysis, Ergonomics.

I. INTRODUCTION

Enhancing performances of technical gestures has always been a great concern for human beings. Such performances consists in a potentially conflicting combination between the achievement of some operational goal, and the minimization of the biomechanical demands experienced by the person. Numerous applications are concerned by such dual-objective performances. At work, the exposure to musculoskeletal disorders (MSD) risk factors is now often considered, in addition to the productivity of the worker, when designing workstations [1], [2]. In sports, coaches aim at finding the right gesture in order to improve athletes' results, while preventing injuries [3], [4]. In rehabilitation (*e.g.* after injury or surgery), knowing what motion patterns alleviate the stress on a weakened body part can help provide exercises or recommendations to prevent further injury [5].

The assessment and improvement of a gesture are usually conducted under the supervision of an expert (ergonomist,

physiotherapist...), who observes the gesture and provide recommendations based on his/her knowledge and experience. However, the availability of experts may be limited (*e.g.* during the design process of a workstation), and besides, observational methods can provide qualitative but no quantitative measures of the biomechanical demands to which a person is exposed during a technical gesture. Therefore, in order to assist and complete the work of experts, digital human software tools have been developed, such as OpenSim [6] or AnyBody [7], in which the human gesture is reproduced with a virtual manikin. Indeed, the use of a virtual manikin enables easy access to detailed force and motion-related biomechanical quantities, which otherwise cannot be measured on real humans, or only with heavy instrumentation (*e.g.* muscle or joint forces). However, such tools do not necessarily guarantee the reliability of the biomechanical quantities measured on the manikin [8]. One key factor is the mapping of the human motion onto the manikin: it should result in a dynamically consistent motion (*i.e.* which respects the laws of physics), but existing software cannot fully guarantee such consistency.

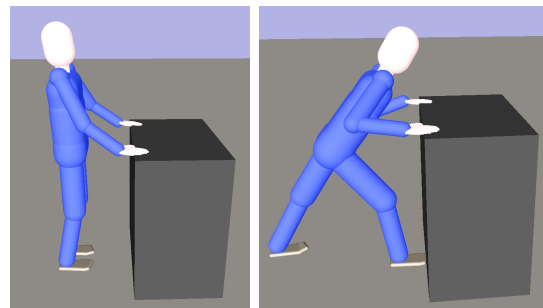


Fig. 1: Two different ways of pushing a heavy object, resulting in different biomechanical demands on the human body (inspired from [9]).

Moreover, beyond the evaluation of an existing gesture, a crucial question is the modification of the way the gesture is performed, in order to improve the performances (Fig. 1). Despite the advances in human biomechanics and modeling tools, such enhancements are still generally achieved through an intensive trial and error process. Indeed, the analytical relation between the macroscopic parameters of the gesture (*i.e.* the parameters defining the way the gesture is performed, and which can be altered) and the resulting performances is often complex. In [9], Demircan proposes a tool for analyzing the relation between the way athletes (novice and experts) perform a gesture and the resulting operational performance, in terms of operational acceleration. This analysis enables to

Pauline Maurice, Vincent Padois and Philippe Bidaud are with Sorbonne Universit s, UPMC Univ Paris 06, and CNRS, UMR 7222, Institut des Syst mes Intelligents et de Robotique (ISIR), F-75005, Paris, France. (e-mail: maurice(at)isir.upmc.fr, vincent.padois(at)upmc.fr, bidaud(at)isir.upmc.fr).

Philippe Bidaud is also with ONERA, 91123 Palaiseau, France.

Yvan Measson is with the Interactive Robotics Laboratory, CEA-LIST, F-91191 Gif-sur-Yvette, France (e-mail: yvan.measson(at)cea.fr).

understand the features which differentiate an efficient gesture from a non-efficient one, but it does not explicitly provide recommendations about how to execute an optimal motion (the analyzed motions are recorded on real subjects, thus still requiring experts). Besides, a single performance criterion is considered, whereas a detailed assessment of biomechanical performances often requires to take several quantities into account (*e.g.* joint loads, joint positions, energy consumption...). Such quantities can be differently affected by a same parameter of the gesture, which requires compromises and renders the identification of a better solution even less straightforward.

This paper presents a method to automatically identify how the performances of a given technical gesture can be improved, from very few input data. The proposed tool consists in two components:

- A method for dynamically replaying pre-recorded human motions, which ensures the dynamic consistency of the resulting motion. Such a replay enables both the acquisition of the technical gesture to execute (*e.g.* trajectories to follow and forces to exert), and the evaluation of an existing situation. The chosen approach relies on an optimization-based controller which enables to track the subject's motion in the operational space, while imposing dynamic and biomechanical constraints (*i.e.* joint and actuation limits).
- A method for analyzing the dependence of the performances on the parameters of the gesture. Such an analysis enables the identification of the parameters which most affect the overall performance, in order to provide recommendations for improving the situation. The proposed approach relies on a virtual human simulation framework, in which a variety of situations can be automatically created and simulated. Thus a sensitivity analysis can easily be conducted, without the need for much input data.

Thanks to these measurement and analysis tools, enhancing the performance of technical gestures is facilitated. The gesture is acquired on the initial situation, and serves as an input for the sensitivity analysis, which results provide recommendations for improvement. The modified situation is then evaluated and compared to the initial situation, in order to verify the positive effect of the proposed modifications.

In this work, the human body is represented with rigid bodies, and does not include muscle actuation: the manikin is actuated by a single actuator at each joint. Indeed, even though muscle-related quantities cannot be estimated with such a model, numerous quantities can still be measured for representing the biomechanical demands that occur during whole-body activities (*e.g.* joint loads, joint dynamics, mechanical energy...). Besides, while musculoskeletal models have proved valid and insightful in some cases, no criterion has been established yet to solve the muscle recruitment problem in general. So the realism of the muscle-related measurements cannot be ensured in all possible whole-body situations [7], [8], [10], [11]. The questionable gain of information, associated with a much more important computational cost, therefore reduces the interest of musculoskeletal models in the current context.

The paper is organized as follows. Section II presents the dynamic replay method. Section III presents the method for analyzing the performances with respect to the gesture parameters. Section IV describes the experimental set-up which is used for validating the proposed methods. The results are presented in section V and discussed in section VI.

II. DYNAMIC REPLAY OF HUMAN MOTION

Virtual manikins are commonly used for estimating biomechanical quantities during the execution of human motions. However, the accuracy of the human gesture reconstruction, both in terms of motion and force, strongly affects the reliability of the measures¹. Human motion is often captured through optical motion capture techniques, in which markers are positioned on the body of the subject, and cameras record the 3D Cartesian positions of the markers. Though mapping of motion capture data onto virtual avatars has been extensively used for several decades, the current mapping techniques still lack physical consistency, especially when the motion is highly dynamic and/or involves significant interaction forces with the environment.

A. Related work

Mapping the recorded human motion onto a virtual manikin is commonly done with inverse kinematics techniques (IK), which convert the markers operational space trajectories into joint space trajectories. With IK, biomechanical quantities such as joint positions or velocities can be measured, but the driving forces (joint torques here) cannot be estimated. Therefore an inverse dynamics (ID) step - in which the driving forces are computed from the dynamic model and the joint space trajectories resulting from the IK - must be performed afterwards. Though widely used, the IK+ID process has several drawbacks. Firstly, the inversion in the IK step requires intensive computations and is therefore time consuming. Secondly, the IK solution is not unique, so the resulting motion may not be plausible. Therefore many studies propose modifications of the IK, so that the resulting motion matches a given set of constraints [12], [13]. However, the dynamic properties of the human body are not considered (such techniques are especially used in computer animation, where the visual realism is the main concern), so the motion computed through IK is hardly ever dynamically consistent. This results in the impossibility to achieve the force equilibrium in the ID step, when the experimental external forces (*e.g.* ground contact forces) are added. For instance, in OpenSim, this inconsistency appears in residual forces [8].

In order to improve the dynamic consistency of the replayed motion, some studies include dynamic considerations in the motion computation process. Some combine IK with dynamic corrections in order to modify motion capture data to respond to physical collision forces [14]. Others directly use controller-based techniques including dynamic constraints to animate

¹The retargetting problem (*i.e.* mapping the motion of a subject onto an avatar with a different morphology) is not considered here. The work presented here assumes that the virtual manikin morphology can be adapted to each subject, and that its kinematics is very similar to the human body kinematics.

the manikin [15], [16]. However, the controller requires the desired joint trajectories as an input, so a preliminary IK step is still needed.

In order to avoid the computationally expensive IK step, John and Dariush [17], Ott *et al.* [18], and Demircan *et al.* [19] propose to work directly in the operational space. In [17], John and Dariush utilize a task space kinematic control method (closed-loop inverse kinematics) and dynamic constraints, to track the motion directly in task space. In [18], Ott *et al.* connect the markers to the manikin body with virtual springs, and use the generated forces to compute the manikin motion through the dynamic model equation. In [19], Demircan *et al.* use an operational space approach based on null-space projection [20] to track the Cartesian markers trajectories. However, all these techniques either omit certain constraints, or they do not take them explicitly into account (especially inequality constraints). They resort to suboptimal heuristic ways to account for inequality constraints through avoidance tasks [21].

B. Virtual human controller

The dynamic replay method proposed in this work is based on a direct control of markers in the operational space, through an optimization-based controller. Contrarily to analytical techniques (explicit null-space projection), such a numerical technique enables to solve the human kinematic redundancy, while considering both equality and inequality constraints. The dynamic and the biomechanical consistency of the resulting motion is thus ensured.

The motion of the manikin is computed with the linear quadratic programming (LQP) controller framework developed by Salini *et al.* [22]. Linear quadratic programming handles the optimization of a quadratic objective that depends on several variables, subjected to linear equality and inequality constraints. The variables here are the joint torques, the contact forces, and the joint accelerations (though the latter could be excluded from the optimization variable and computed with the equation of motion). The recording of the contact forces (especially the ground contact forces) is therefore not necessary to replay the motion, which is a significant advantage compared to IK+ID methods, since it simplifies the experimental set-up. The control problem is formulated as follows:

$$\begin{aligned} & \underset{\mathbb{X}}{\operatorname{argmin}} \quad \sum_i \omega_i T_i(\mathbb{X}) \\ & \text{s.t.} \quad \begin{cases} M(\mathbf{q})\ddot{\mathbf{q}} + \mathbf{C}(\mathbf{q}, \dot{\mathbf{q}}) + \mathbf{g}(\mathbf{q}) = S\boldsymbol{\tau} - \sum_j J_{c_j}^T(\mathbf{q})\mathbf{w}_{c_j} \\ G\mathbb{X} \preceq \mathbf{h} \end{cases} \end{aligned} \quad (1)$$

where $\boldsymbol{\tau}$ is the joint torques, \mathbf{w}_c the contact forces, \mathbf{q} the generalized coordinates of the system, with $\dot{\mathbf{q}}$ and $\ddot{\mathbf{q}}$ its first and second derivatives, and $\mathbb{X} = (\boldsymbol{\tau}, \mathbf{w}_c, \ddot{\mathbf{q}})^T$. The equality constraint is the equation of motion: M is the inertia matrix of the system, \mathbf{C} the vector of centrifugal and Coriolis forces, \mathbf{g} the vector of gravity forces, S the actuation selection matrix, and J_c^T the Jacobian of contacts. The inequality constraint includes the bounds on the joint positions, velocities, and

torques (all formulated with $\boldsymbol{\tau}$ and $\ddot{\mathbf{q}}$), and the contact existence conditions for each contact point, according to the Coulomb friction model:

$$\begin{aligned} C_{c_j} \mathbf{w}_{c_j} &\leq 0 \quad \forall j \\ J_{c_j}(\mathbf{q})\ddot{\mathbf{q}} + \dot{J}_{c_j}(\dot{\mathbf{q}}, \mathbf{q})\dot{\mathbf{q}} &= 0 \quad \forall j \end{aligned} \quad (2)$$

where c_j is the j th contact point, C_{c_j} the corresponding linearized friction cone, and \mathbf{w}_{c_j} the contact wrench.

The objective function is a weighted sum of tasks T_i representing the squared error between a desired acceleration or wrench and the system acceleration/wrench (ω_i are the weighting coefficients). The solution is then a compromise between the different tasks, based on their relative importance². The following tasks are defined:

- Operational space acceleration $\|J_i \ddot{\mathbf{q}} + \dot{J}_i \dot{\mathbf{q}} - \ddot{\mathbf{X}}_i^*\|^2$
- Joint space acceleration $\|\ddot{\mathbf{q}} - \ddot{\mathbf{q}}^*\|^2$
- Operational space wrench $\|\mathbf{w}_i - \mathbf{w}_i^*\|^2$
- Joint torque $\|\boldsymbol{\tau} - \boldsymbol{\tau}^*\|^2$

where $\ddot{\mathbf{X}}_i$ is the Cartesian acceleration of body i , and \mathbf{w}_i the wrench associated with body i . The superscript $*$ refers to the desired acceleration/force, which are defined by a proportional derivative control. For instance, the desired acceleration is:

$$\ddot{\mathbf{X}}^* = \ddot{\mathbf{X}}^{\text{goal}} + K_v(\dot{\mathbf{X}}^{\text{goal}} - \dot{\mathbf{X}}) + K_p(\mathbf{X}^{\text{goal}} - \mathbf{X}) \quad (3)$$

where K_p and K_v are the proportional and derivative gains. The superscript *goal* indicates the position, velocity and acceleration wanted for the body or joint.

C. Tasks for motion replay

In order to track the markers trajectories, an operational acceleration task is created for each marker positioned on the subject/manikin's body (Fig. 2). The reference trajectory corresponds to the recorded marker trajectory. Depending on the total number of markers and their respective placement on the subject, the problem can be over constrained (*i.e.* not all markers trajectories can be accurately followed). However, the weighting strategy of the LQP controller allows to deal with conflicting objectives. Nevertheless, the weights of the different markers tasks must be wisely chosen, since they affect the resulting motion. The markers tasks are not all assigned the same weight: the markers associated with distal bodies are given the largest weight, and the weight decreases when the body on which the marker is set is further away from the extremities (in accordance with the recommendations of Demircan *et al.* [19]). Extremities are more affected by cumulative errors on the preceding joint positions, so assigning the largest weights to the operational position tasks of the limb extremities tends to reduce this bias.

The markers tracking tasks are generally not sufficient to maintain the balance of the manikin, especially in motions where the balance is strongly solicited. Indeed, without any

²More generally, any optimization-based controller which enables to properly consider all kinds of constraints can be used, whether the tasks are ordered with a weighting strategy like here, or with strict priorities, such as hierarchical quadratic programming [23].

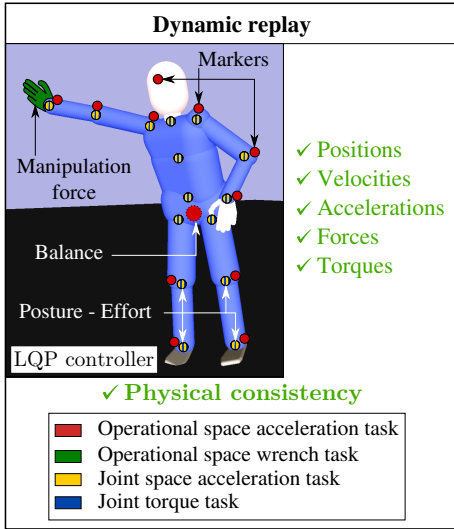


Fig. 2: Joint space and operational space tasks used in the LQP controller for dynamically replaying human motion.

balance task, the balance control is only an open-loop control (the manikin is not instructed to keep its balance). Due to the imprecisions in the human model and markers positions measurements, the open-loop balance control generally results in the fall of the manikin. A balance task is therefore added in the controller, through a center of mass (CoM) task. The reference CoM acceleration is obtained from the CoM jerk computed using a ZMP preview control method³ [24]. Given the non strict hierarchy between the tasks, the balance task may alter the markers tracking tasks. So the weight of the balance task results from a compromise between the accuracy of the replay and the balance preservation. Such a compromise is achieved by giving the balance task a weight smaller than the distal extremities markers tasks.

If an intentional force is to be exerted on the environment by the manikin hand (e.g. pushing an object), an operational force task is created. The reference force must be given as an input to the controller (e.g. thanks to a force sensor measurement). The hand force task weight is similar to the distal markers tasks weights.

Low weight joint position tasks are added to define a natural reference posture (standing, arms along the body) which should be adopted by the manikin when no specific activity is performed. It ensures a rather natural motion in case some bodies are not entirely constrained by the markers tasks.

Finally, joint torque tasks are added for each joint. They aim at minimizing the joint torques to prevent useless effort, and ensure the uniqueness of the solution to the optimization problem. The weights of these tasks are the smallest since they must not hinder the other tasks.

³The original ZMP preview control scheme is slightly modified in this work, so that it takes into account known external forces which affect the manikin balance.

III. SENSITIVITY ANALYSIS OF HUMAN PERFORMANCES

Thanks to the dynamic replay method described in the previous section, performances (operational and biomechanical) can be measured with the virtual manikin. However, these measurements do not provide any hints about how to modify the gesture for enhancing the overall performances. In order to provide such recommendations, the influence of the gesture parameters on the performances must be known. Since no straightforward analytical relation between parameters and performances can generally be established, a statistical sensitivity analysis must be conducted [25].

A. Method overview

Statistical sensitivity analyses rely on the numerical evaluation of the output (here the indicators of performance) for many values of the input parameters. Having a real subject execute the gesture in each situation would be too time consuming, since sensitivity analyses often require a large number of trials. Furthermore, if recommendations are to be provided not for one specific subject, but for subjects of different morphologies (e.g. workers in an industrial plant), parameters representing the diversity of subjects should be added, so as to ensure that human features do not have a strong impact on the results⁴. Given that the purpose of the present work is not to establish general guidelines on how to perform some kinds of gestures, but to provide a tool for easily analyzing any given gesture, the execution of the gesture is rather simulated with an autonomous virtual manikin. Indeed, the virtual manikin enables to test a lot of situations, including different human morphologies, without the need for any human subjects.

The whole process for analyzing the dependence between the parameters of the gesture and the performances can be summarized as follows (Fig. 3):

- 1) Define the parameters which characterize the way the gesture is performed, and which can be altered (and possibly the human parameters as well).
- 2) Select, among all the possible combinations of parameters values, those that should be tested.
- 3) Simulate the execution of the activity with the virtual manikin, for each selected combination of parameters values, in order to measure the indicators of performance.
- 4) Compute sensitivity measures for the performance indicators, based on their values in all the tested cases.

Step 1 depends on the gesture which is studied and is therefore left to the user. Steps 2 and 4 are detailed in the following sections. The simulation step 3 is performed with an autonomous virtual manikin (i.e. no motion capture). The manikin is animated with the same LQP controller as the one used for the motion replay (see section II-B), but the tasks included in the controller are slightly different. The markers tracking tasks are removed, and replaced by a hand (and possibly other body parts, depending on the gesture)

⁴Otherwise, morphology-specific recommendations should be provided, possibly with modifications of the environment (e.g. adjustable parts in a workstation).

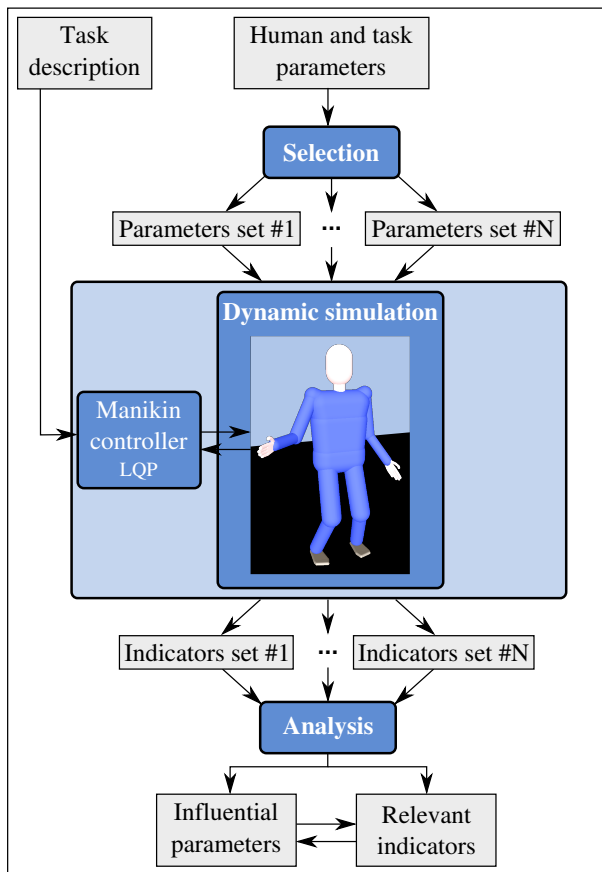


Fig. 3: Flow chart of the method for analyzing the dependence between parameters of the gesture and resulting operational/biomechanical performances.

operational acceleration task. The reference trajectory - and force profile if required - of the hand task is either obtained from the motion recorded on a human subject (especially if a very specific trajectory must be followed), or it can be interpolated from start and end points defined by the user (for instance, in less specific gestures such as reaching motions).

B. Parameters space exploration

The parameters which represent the way the gesture is performed take continuous values, so they must be discretized to form the different combinations of parameters values to be tested. However, though it depends on the length and complexity of the activity that is simulated, the computational cost of a simulation is always quite expensive: with most physics engine based robotic simulators, simulations cannot run faster than real time, and in many cases (multiple contacts, many tasks in the manikin controller...), the simulation is even slower. Therefore the number of situations which are tested is limited and the values of the parameters must be carefully selected.

Optimizing the exploration of the parameters space requires a compromise between the number of trials and the precision of the resulting information, and is therefore strongly influenced by the objective of the study [25]. In this work, the analysis aims at quantitatively estimating the influence of each

parameter on the performance indicators, in order to identify which parameters should mainly be modified. The computation of Sobol indices, which relies on the decomposition of the output variance of the considered function (functional ANOVA decomposition), is then well adapted⁵ [26], [27]. Indeed, Sobol indices allow a precise ranking of the influence of the different parameters, without requiring specific hypotheses on the monotony of the performance indicators. Furthermore, their interpretation is quite straightforward: each index measures the percentage of variance of an indicator that is explained by the corresponding parameter(s).

The first order indices S_i represent the variance of a performance indicator explained by one single parameter X_i (no interaction). Indices of superior order consider the interactions between parameters. The total indices S_{T_i} represent all the effects of X_i on the indicator, including all interactions with other parameters. The first order and total indices are of particular interest for ranking the parameters, since they give information about the i th parameter, independently from the influence of the other parameters. A high S_i means that X_i alone strongly affects the performance indicator, whereas a small S_{T_i} means that X_i has very little influence on the indicator, even through interactions. Only these indices are considered in this work. The mathematical definition of Sobol indices is given in appendix A.

The extended FAST (Fourier amplitude sensitivity testing) spectral method is used for choosing the appropriate parameters values to test, and for computing Sobol indices [28]. The exploration method used for the FAST analysis is a good compromise between the comprehensiveness of the space exploration (FAST uses space-filling paths) and the number of trials (about one thousand trials per parameter, whereas Monte Carlo methods - the main alternative for the computation of Sobol indices - often requires about ten thousand trials per parameter).

C. Performances analysis

Once the simulations are performed for all the selected combinations of parameters values, Sobol indices can be computed. However, Sobol indices only address single-output models, whereas the performances of a gesture are often evaluated with several indicators with different meanings. For instance, a detailed assessment of the biomechanical performances requires one indicator per kind of biomechanical demand: position, effort, energy... for the different body parts. Even though Sobol indices can be computed separately for each indicator, no global sensitivity index can be obtained for a parameter by aggregating the indices relative to different indicators (the comparison of the indices referring to different indicators is meaningless). Therefore, in order to estimate the global influence of a parameter on the overall performance of the gesture, the most relevant performance indicators must first be identified.

⁵If the number of parameters is too large, (typically more than a dozen), a preliminary screening analysis can be performed to eliminate parameters with very little influence. A more detailed analysis can then be conducted on a reduced number of parameters only.

In the context of performance improvement, the relevance of an indicator is not related to its value, but to its variations when the gesture is performed in different ways. Indeed, if the value of an indicator remains unchanged, whichever the way the gesture is performed, this indicator is not useful to compare different executions of the gesture. Furthermore, many indicators only give a relative information (no absolute reference value is available to determine an absolute level of risk), therefore, the value in itself is meaningless.

The problem of reducing the number of performance indicators to keep only the ones that best explain the disparity has been addressed by Campbell *et al.* [29] and Lamboni *et al.* [30] in the context of sensitivity analysis for multiple-output models. They propose to decompose the model outputs in a well-chosen basis before applying sensitivity analysis to the most informative components individually, which comes down to a dimensionality reduction problem. However most dimensionality reduction methods form composite variables (*i.e.* combinations of the initial variables), which would result in physically meaningless results here. Indeed, the original indicators potentially have very different physical meanings, and the influence of a parameter may vary much from an indicator to another. So standard dimensionality reduction methods (such as principal components analysis) cannot be used. Instead the importance of each performance indicator is represented directly by its variance. The indicators can thus be ordered, and the most discriminating ones (*i.e.* those with the highest variance) can easily be identified. A sensitivity analysis can then be performed separately for each one of the most discriminating indicators. The sensitivity indices relative to different indicators still cannot be compared, however the overall number of indices is reduced, making the interpretation of the results easier for the user.

Before ranking the performance indicators based on their variance, they must be scaled because they have non-homogeneous units. Therefore they do not have the same order of magnitude, so they cannot be compared as such. In standard dimensionality reduction methods, this is often done with the variables standard deviation, but then the scaled variables all have a unit variance. Since the variance is precisely what represents the indicators global sensitivity to the gesture parameters, this scaling would result in the loss of relevant information. Another option is to use physiological limit values relative to each indicator for the scaling. However, some indicators do not have well-defined limits. Instead, the order of magnitude of an indicator can be roughly estimated by measuring the indicator in many different situations (which is quite easy with the virtual manikin simulation), and taking its average value. If gestures of many different kinds are considered and performed in many different ways, it can be assumed that the range of values of each indicator is covered quite exhaustively.

Depending on what they represent, performance indicators may be measured for each time step of the simulation (*e.g.* joint loads). However, the ranking method described here - as well as the computation of Sobol indices - requires that each indicator (for each situation) is represented by a single value. The indicator must then be summarized in a single value, *e.g.* with its time-integral value on the whole duration of the

gesture, or its maximal value.

Once the performance indicators are ranked according to their variance, the number of indicators that are kept must be decided. The objective is to limit the number of indicators that are considered, while sufficiently accounting for the global performance of the gesture. This problem is similar to selecting the number of dimensions in principal components analysis, therefore a related criterion - the Scree test - is used [31]. The variance associated with each indicator is plotted in decreasing order. The curve first drops, then makes an elbow toward less steep decline. Only the indicators before the curve elbow (usually excluding it) are kept.

IV. EXPERIMENTAL SET-UP

The whole method for guiding the performance enhancement of a gesture, presented in the previous sections, is applied to a real gesture. Firstly, the motions of human subjects are recorded and replayed, in order to evaluate the consistency of the proposed replay method. Part of the recorded gesture is then used as an input for the sensitivity analysis, which is conducted to identify the discriminating performances indicators and the influential parameters. Based on these results, recommendations on how to improve the performances of the gesture are provided. The modified gesture is then compared to the original one, in order to ensure that the proposed recommendations indeed enhance the performances, and thereby to demonstrate the usefulness of the proposed method.

A. Task description

The gesture considered in this experiment is an industrial manual task which requires non-negligible efforts, and in which the main concern are ergonomic performances. The task consists in drilling six holes consecutively in a vertical slab of autoclaved aerated concrete, with a portable electric drill. The locations of the holes are imposed, and depicted on Fig. 4. They are chosen so that the task demands significant changes in the subjects' posture, yet remains feasible without feet motion.

The drill weights 2.1 *kg*. The average normal force needed to drill a hole in these conditions is about 40 *N*. There is no constraint on the task duration, however it takes about 1 min to perform the whole task: take the drill, drill the six holes, and put the drill down.

B. Motion capture set-up

1) *Subjects*: Five right-handed healthy subjects (3 males and 2 females) ranging from 25 to 30 years old take part in the experiment. Their average height is 1.72 *m* (SD 0.1, min 1.53, max 1.82), and their average body mass index is 22.6 *kg.m*⁻² (SD 0.8, min 21.7, max 23.8). Each subject performs the task ten times, with a resting period between each performance. The subjects choose their feet positions, and are allowed to change them between each performance. However, they are instructed not to move their feet during one performance. The drill is held with the right hand only. Before starting the experiment, the subjects train several times in order to find a comfortable feet position, and to limit the learning effect during the recording.

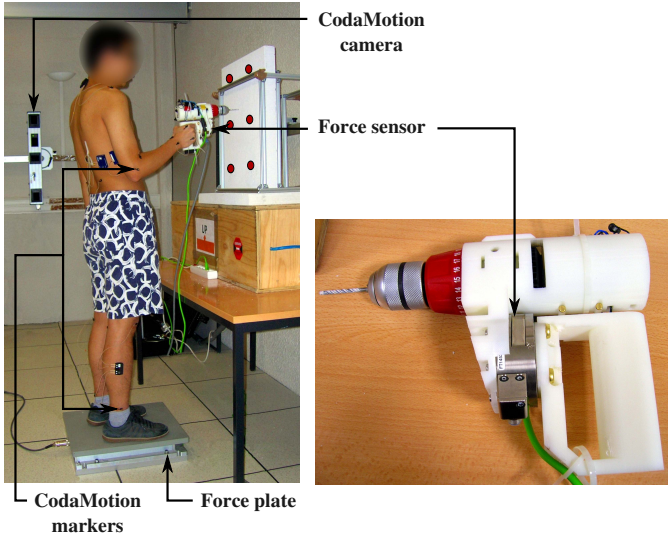


Fig. 4: Motion and force capture instrumentation for the drilling task. A commercial drill has been modified in order to embed a force sensor. The red circles on the slab represent the drilling points.

2) *Instrumentation*: The subjects' motions are recorded with a CodaMotion⁶ system. The subjects are equipped with 25 markers spread all over their body (both legs, both arms, back and head). They stand on an AMTI force plate⁷ while performing the task, in order to measure the contact forces with the ground. A 6 axes ATI force sensor⁸ is embedded in the drill handle, in order to measure the drilling forces. The drill is equipped with 3 CodaMotion markers so that the force sensor position and orientation is known. The acquisitions of the force sensor, the force plate and the CodaMotion data are synchronized thanks to an external trigger. The instrumentation used to record the forces and motions is displayed in Fig. 4. The recorded CodaMotion and force sensors data are filtered with a zero-phase 10 Hz low pass 4th order Butterworth filter (no delay is introduced between the raw and the filtered data). The markers velocities and accelerations are then computed from the markers positions with finite differences.

3) *Replay*: The motions recorded on the human subjects are replayed with the manikin and the LQP controller, according to the dynamic replay method described in section II. In addition to the markers tracking tasks, the balance task, the postural task and the joint torque minimization task, an operational force task is added for the right hand (same weight as the wrist markers tasks). This force task corresponds to the drilling force: its reference value is provided by the measures from the force sensor. On the contrary, the ground contact forces measured with the force plate are not used in the simulation, since they are automatically computed by the manikin controller. The experimental values are used for validation purpose only.

The simulations are run in the XDE⁹ dynamic simulation framework, developed by CEA-LIST [32]. The XDE manikin

consists of 21 rigid bodies linked together by 20 compound joints with a total of 45 degrees of freedom (DoF), plus 6 DoFs for the free floating base. Each DoF is a revolute joint controlled by a sole actuator. Given a subject size and mass, the manikin is automatically scaled according to average anthropometric coefficients. Each body segment can be further manually modified to match the subject morphology when needed.

C. Sensitivity analysis set-up

1) *Parameters*: Given the considered activity, the parameters which can be modified are mostly related to the position of the person relative to the work area, and to posture-related preferences. Nine parameters are defined (including parameters related to the person's morphology), and are listed in table I.

Parameter	Min.	Max.
person's height (m)	1.65	1.85
person's body mass index ($kg.m^{-2}$)	21.0	27.0
reference position for elbow flexion ($^{\circ}$)	10	135
drill handle orientation in slab plane / vertical ($^{\circ}$)	0	90
stab center height / shoulder height (m)	-0.2	0.1
offset distance pelvis - center of stab (m)	-0.3	0.0
angle pelvis - normal to stab ($^{\circ}$)	-30	30
inter-feet distance in frontal plane (% of hip width)	100	200
inter-feet distance in sagittal plane (m)	-0.25	0.25

TABLE I: Parameters minimum and maximum values. The pelvis position is given in polar coordinates with respect to the center of the stab. The offset for the pelvis-stab distance is added to the manikin arm length to define the real pelvis-stab distance. The right foot is at the front when the feet distance in the sagittal plane is positive.

The choice of the parameters values for the extended FAST analysis is generated through the R software¹⁰. The sample size and set of frequencies (depending on the number of input parameters) are chosen according to the recommendations of Saltelli *et al.* [28]. It results in a total number of 11601 trials. One simulation takes approximately 2 min total (the real activity lasts 75 s), on one core of a 2.4 GHz Intel R CoreTM i7 laptop, and the simulations can be parallelized.

2) *Simulations*: The drilling activity is simulated with the autonomous virtual manikin (in the XDE framework as well), animated with the LQP controller. The following tasks are included, in decreasing order of importance: balance, right hand trajectory and force, gazing, posture and torques minimization. An average hand reference trajectory - as well as profile and magnitude of the drilling force - are estimated from the data of the five human subjects. The position of the manikin feet are imposed and are not supposed to move during the simulation (except if the dynamic balance cannot be maintained and the manikin falls).

3) *Performance indicators*: Ergonomic indicators aim at quantifying the effects of the physical demands on the worker. Most ergonomic assessment methods exclude dynamic phenomena though they also generate MSD [33], [34]. Here on the contrary, the following biomechanical quantities are measured

⁶www.codamotion.com

⁷<http://www.amti.biz/>

⁸http://www.ati-ia.com/products/ft/ft_models.aspx?id=Gamma

⁹www.kaliteo.fr/lisi/en/aucune/a-propos-de-xde

¹⁰<http://www.r-project.org>

thanks to the dynamic simulation framework: *joint position, velocity, acceleration, power and torque*. Similarly to what is done for robot manipulators [35], each one of these quantities is then summed up on all the joints of a given body part, in order to form more synthetic performance indicators. The mathematical form of a indicator is

$$\frac{1}{p} \sum_{i=1}^p (s_i)^2 \quad (4)$$

where s_i is the biomechanical quantity (position, velocity...) of joints i , and p the number of joints in the considered body part: torso, right arm, left arm, or legs. When physiological limit values are available, s_i is normalized by its limit value s_i^{max} before the summing [34]. However these limits are strongly person-dependent, and maximum values are often not well-documented in the literature (e.g. joint velocities or accelerations), making the normalization impossible.

In addition to these local indicators, global quantities which represent the ability of the person to comfortably perform certain actions are considered. The balance is estimated through two indicators: the *sum of the square distances between the ZMP and the base of support boundaries (balance stability margin)* [36], and the *time before the ZMP reaches this boundary (dynamic balance)*, assuming its dynamic remains the same. The first quantity represents the capacity to withstand external disturbances, whereas the second evaluates the dynamic quality of the balance. The capacity to produce force (resp. movement) in a given direction is evaluated with the *force (resp. velocity) transmission ratio of the right hand* proposed by Chiu [37], except that the dynamic manipulability [38] is used instead of the kinematic one. The considered directions are the drilling and motion directions. Eventually the *kinetic energy* of the whole body is added to the indicators list. All the global indicators (except the kinetic energy) should be maximized in order to improve the situation, whereas the local indicators should be minimized. For the sake of homogeneity, the inverse value is considered when needed, so that a good ergonomic situation always corresponds to a small value of the indicator.

In order to summarize each one of these time-dependent indicators with a single value, the time-integral value over the whole gesture is used. Besides, the reference values used for the scaling are estimated with the average values of the indicators measured on a set of different gestures, performed in different ways¹¹ (such as walking, bending, reaching, following trajectories, pushing and carrying objects) [39].

V. RESULTS

The comparison of the recorded and replayed motions, the output of the sensitivity analysis, and the comparison of the initial and modified gestures are presented and discussed hereafter.

¹¹A video of the some of the corresponding simulations is available here: http://pages.isir.upmc.fr/~padois/website/fichiers/videos/maurice_humanoids_2014.mp4

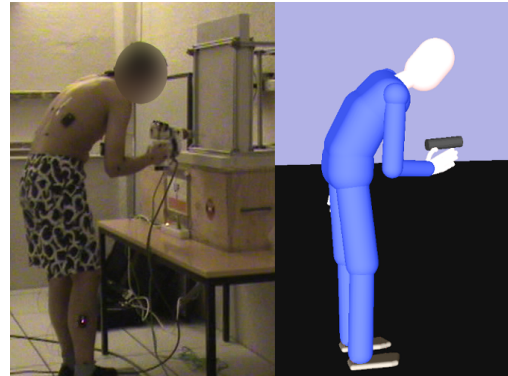


Fig. 5: Motion capture (left) and dynamic replay with the LQP controller (right) of the drilling activity.

A. Dynamic replay validation

The consistency of the replay (Fig. 5) is evaluated regarding both the motion and the forces. The reliability of the replayed motion is evaluated through the comparison between the experimental (recorded with the CodaMotion) and simulated (points on the manikin body for which tracking tasks have been created) markers positions. The reliability of the force data should be estimated through the comparison between the manikin joint torques computed with the controller, and the joint torques measured on a human subject (via the muscle forces). However, such measurements on a real subject are hardly possible in practice. On the contrary, the contact forces exerted by a human subject on its environment (e.g. the ground) are easily measured, and they are linked to the joint torques through the equation of motion (equality constraint in Eq. 1). So, provided that the human model and the joint motion are known, the measurement of the contact forces enables an indirect estimation of the joint torques. The force validation therefore focuses on the comparison between the experimental (measured through the force plate) and simulated (computed with the manikin controller) ground contact forces. The results are presented and discussed hereafter¹².

1) *Motion*: The RMS errors between the experimental and simulated markers positions are presented in table II, for each subject. The tracking error is globally small - less than 3 cm for almost all joints - and there is no significant differences between the subjects. The tracking error is the smallest for the distal parts of the body (ankle, hand and head), which is in accordance with the tasks weights distribution used in the controller (higher weights for the distal body parts).

The tracking is much better for the left arm than for the right arm, because the left arm does not move much, whereas the motion of the right arm is significant: the overall length of the right hand trajectory is about 1 m. A tracking error around 1 cm (for the right hand) is therefore satisfying. On the contrary, the tracking error of the right shoulder is not insignificant. One reason to this error is the deformation of the human skin - on which the markers are set - during gestures including a

¹²A video of the recorded and replayed motions is available here: http://pages.isir.upmc.fr/~padois/website/fichiers/videos/maurice_drilling_dyn_replay.mp4

	Position RMS error (cm)						
	S_1	S_2	S_3	S_4	S_5	Mean	SD
Ankle	1.5	1.0	0.9	1.1	1.3	1.2	0.2
Knee	4.6	4.9	3.7	3.8	4.8	4.4	0.5
Back	2.9	3.2	1.7	2.5	3.1	2.7	0.5
Head	1.6	1.6	0.6	1.5	1.0	1.3	0.4
R. Shoulder	7.8	6.9	2.0	6.8	7.0	6.1	2.1
L. Shoulder	3.9	2.7	1.9	2.2	3.5	2.8	0.8
R. Elbow	2.9	3.0	2.7	2.9	3.1	2.9	0.1
L. Elbow	0.8	0.5	0.3	0.8	0.7	0.6	0.2
R. Wrist/Hand	0.8	1.0	1.5	0.7	1.3	1.1	0.3
L. Wrist/Hand	0.5	0.4	0.2	0.3	0.2	0.3	0.1

TABLE II: RMS errors between the experimental and simulated 3D positions of the markers, for each joint and each subject (S_i stands for *subject i*, L for *left* and R for *right*). For each subject, the value displayed is the average value of the ten trials. For each joint, the value displayed corresponds to the biggest error of all markers placed on the corresponding body/joint (the error is approximately the same for all markers placed on a same joint).

wide range of joint motions (right shoulder and elbow here). This deformation results in a variation of experimental inter-markers distances which can reach several centimeters. Since the tracking tasks of the elbow markers are given higher weights than the shoulder marker task, the variation of the inter-marker distance is almost entirely transmitted to the shoulder position. Another reason to the significant shoulder tracking error may be the complexity of the human shoulder joint [40], which is only roughly modeled in the current manikin kinematics.

The tracking error of the knee markers is particularly big, given the small overall displacement of these markers during the drilling activity. This is very likely due to the balance task in the controller, which affects the execution of the other tasks, due to the non-strict priority between the tasks. Due to the imprecisions in the human model, and the markers placement, and the lack of decision skills of the manikin regarding how to recover balance, the ZMP preview control scheme in the balance task is tuned to be quite conservative. Most unstable situations are thus avoided, as long as the original motion itself is not too unstable. However, the balance improvement is achieved only at the cost of a modified motion, hence of a less accurate replay. The knee markers and, to a lesser extent, the back markers are the most affected because the feet and arms Cartesian positions are either fixed or strongly constrained by high weight tasks, so the balance regulation is mainly carried out with the pelvis.

Though evaluated through Cartesian position errors, the similarity observed between the experimental and replayed motions is also valid at joint level, given the high number of markers that are positioned all over the human body. Moreover, since the position errors remain quite small even during dynamic motions, the joint velocities and accelerations are also likely to be quite similar to those of the human subjects. Therefore, the replayed motion is overall very similar to the original one, as long as the balance is not strongly solicited: reliable motion-related biomechanical quantities are measured on the virtual manikin. Nevertheless, the data measured on

	Force			Moment		
	F_X	F_Y	F_Z	M_X	M_Y	M_Z
Subject No.1	0.82	0.98	0.70	0.78	0.98	0.96
Subject No.2	0.82	0.98	0.62	0.95	0.98	0.95
Subject No.3	0.62	0.98	0.57	0.96	0.98	0.96
Subject No.4	0.78	0.98	0.91	0.96	0.98	0.98
Subject No.5	0.77	0.98	0.82	0.96	0.98	0.97
Average	0.76	0.98	0.72	0.92	0.98	0.97
SD	0.07	0	0.13	0.07	0	0.01

TABLE III: Pearson's correlation coefficient between the ground contact forces computed with the manikin controller and those measured experimentally. Y is the drilling direction, and Z the vertical. For each subject, the value displayed is the average value of the ten trials.

the manikin remain approximations of the reality, since the manikin kinematics is a simplified version of the human kinematics, and since the controller does not ensure that the tasks are entirely fulfilled. Therefore, the virtual manikin simulation does not enable a fine comparison of situations which are quite close. The small differences between the two situations may as well come from model or controller inaccuracies, as from real differences in the gesture.

2) *Forces and Moments*: In the simulation, the contact surface between the manikin foot and the ground is approximated by several contact points distributed under the foot. However the force plate only measures the global contact wrench, so all the contact forces from the simulation (*i.e.* computed in the controller) are gathered to form the global equivalent contact wrench. It should be noted that, though the value of the foot/ground friction coefficient in the simulation is only an approximation of the real value, it has no consequences on the force values. Indeed, the ratio between the tangential and normal forces is always far smaller than the sliding limit for the considered materials.

In order to quantify the similitude between the experimental and simulated data, the Pearson's (linear) correlation coefficients are summarized, for each subject, in Table III. A good correlation - Pearson's coefficient ≥ 0.70 (0.90 for four of the components) - is observed for each component of the contact wrench. Furthermore, as depicted in Fig. 6, no significant permanent force/moment offset (*i.e.* vertical offset on the graphs) is observed. Among the force components, F_Y (direction of drilling) shows a far better correlation than F_X and F_Z , because the amplitude of its variations is much bigger (see Fig. 6 for typical ranges of variation of the forces and moments in the drilling task). Besides, except for the vertical force F_Z , there is no significant differences between the subjects. The disparity of the F_Z results is partly caused by a lower precision of the force plate in this direction, because of the higher load: the ratio between the average measurement precision (about $\pm 0.1\%$ of the applied load for each axis) and the range of variation of the force/moment is smaller than 10^{-3} for F_X , F_Y , M_X , M_Y and M_Z , whereas it is around 0.15 for F_Z .

Since the manikin joint torques result from the dynamic motion equation (equality constraint in Eq. 1), they are affected by the external forces, the kinematic and dynamic properties of the manikin model (coefficients of the M matrix and the

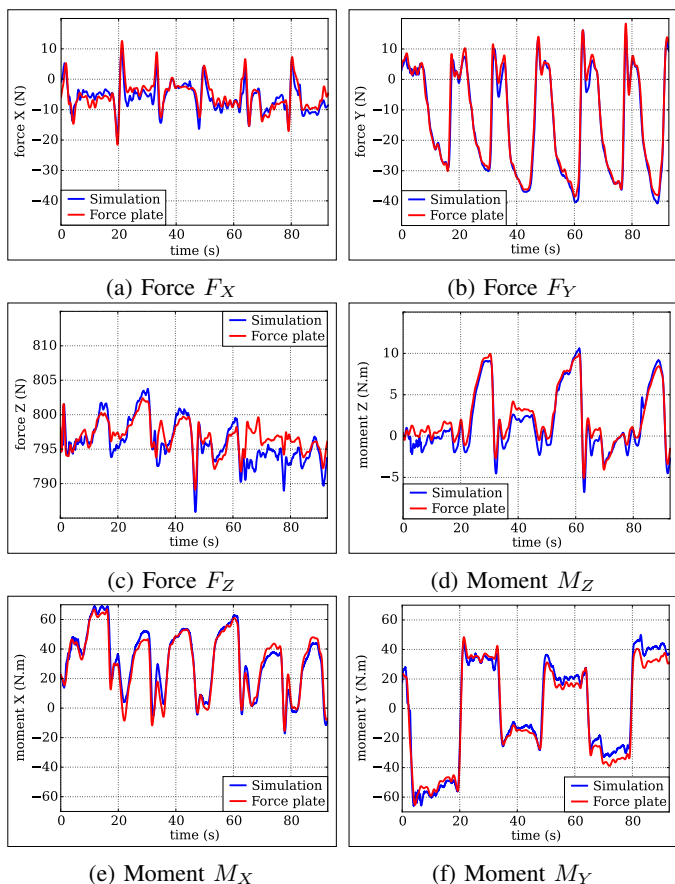


Fig. 6: Time evolution of experimental and simulated components of the ground contact wrench, for one trial of subject No.5. The moments are expressed at the center of both feet. The subject and trial are chosen so that the force and moment errors are representative of their average values over all the subjects and trials.

\mathbf{C} and \mathbf{g} vectors), and the joint motions. The length and mass distributions of the manikin model coming from standard values, the coefficients of M , \mathbf{C} and \mathbf{g} can be assumed quite consistent. Then, according to the motion-related results, the replayed joint motion is quite similar to the original one. Finally, the simulated external forces are mostly consistent with the experimental ones. Therefore, the manikin joint torques computed with the LQP controller during the dynamic replay are considered consistent with the human joint torques.

B. Sensitivity analysis

Table IV summarizes the ergonomic indicators that are identified as relevant according to the proposed analysis, as well as Sobol first order and total indices corresponding to these indicators. Six ergonomic indicators are identified as discriminating, out of 27 indicators in the initial list. These six indicators together represent 80% of the total variance information, therefore only little information is lost by not considering the other indicators. The selection of the upper-body torque (right arm and back) and position (right arm) indicators is not surprising, given that the activity requires the

exertion of a non-negligible force with the right hand, while covering a quite extended area (25×50 cm). The absence of any velocity or acceleration indicators seems consistent with the fact that the drilling activity does not require fast motions.

Some parameter-indicator relations - obtained through Sobol indices - are strongly expected, and confirm the consistency of the proposed analysis. For instance, inter-feet distances (in both directions) strongly affect the balance stability, since they modify the size of the base of support. However, the proposed analysis also highlights some less straightforward phenomena. The back torque indicator and the right arm position and torque indicators are much more affected by the pelvis orientation relative to the stab, than by the orientation of the drill handle or the desired elbow flexion. This may be due to the joint and actuation limits in torsion being much smaller than in flexion (the indicators being calculated as distances to those limits). The legs position indicator is significantly affected by the elbow flexion: the legs are probably used for compensating for the difference in the arm reach by moving the pelvis forward or backward. The stab height has very little effect on any of the relevant indicators. This might however be due to the chosen range of variation of the stab height which is quite small compared to the vertical dimension of the drilling area.

In order to enhance the ergonomic performances, the pelvis orientation, the inter-feet sagittal (and to a lesser extent frontal) distance, and the desired elbow flexion, should primarily be considered, since they have a significant influence on the discriminating indicators. On the contrary, the stab height and the pelvis-stab distance have little influence (small values of Sobol total indices), so their values can be freely chosen by the person performing the activity, depending on what he/she finds more convenient. The human features also have little effect on the performances, so recommendations can be provided independently from the person's morphology.

Sobol indices provide quantitative information on the importance of the parameters effects on the indicators, but, they do not inform on the evolution of the indicators vs. the parameters¹³. However, given the large number of trials that are performed for the sensitivity analysis, trend curves can be plotted and used to roughly identify optimal parameters values. For each parameter, only the indicators which are significantly affected are considered. Nevertheless, compromises may be necessary if different indicators correspond to different optimal parameter values (*e.g.* for the elbow flexion). In such cases, the indicators ranking can be considered to guide the compromise. Recommendations for all seven parameters (excluding the person's morphology) are provided in table V.

C. Validation of the gesture modification

In order to validate the benefit resulting from the proposed recommendations, the modified gesture is compared to the initial one. As a first validation, the modified gesture is evaluated through an autonomous simulation, since it does not require any human subject and is therefore much faster

¹³In order to estimate such evolution, a metamodel can be used [41], however building a metamodel requires many more trials.

		Relevant ergonomic indicators					
		Right Arm torque	Legs position	Right Arm position	Back torque	FTR drilling direction	Balance stab. margin
		23 %	20 %	15 %	9 %	7 %	6 %
Parameters	Person's height	10^{-3} 0.02	0.01 0.35	10^{-3} 0.04	0.02 0.10	0.09 0.11	0.03 0.05
	Person's bmi	10^{-4} 0.03	10^{-3} 0.31	10^{-4} 0.10	0.01 0.10	0.26 0.30	10^{-4} 0.03
	Elbow flexion	0.22 0.26	0.11 0.67	0.03 0.08	10^{-3} 0.09	0.02 0.06	10^{-3} 0.03
	Drill orientation	0.16 0.26	10^{-4} 0.32	0.16 0.24	10^{-3} 0.12	10^{-3} 0.05	10^{-4} 0.02
	Stab height	0.04 0.09	10^{-4} 0.26	0.05 0.09	0.06 0.20	0.04 0.07	10^{-4} 0.02
	Pelvis distance	0.09 0.15	0.01 0.30	0.06 0.19	0.01 0.10	0.04 0.08	10^{-4} 0.03
	Pelvis angle	0.32 0.37	0.02 0.50	0.45 0.59	0.43 0.63	0.45 0.52	0.10 0.19
	Feet sagittal distance	0.01 0.03	0.16 0.66	0.08 0.15	0.15 0.30	10^{-3} 0.02	0.17 0.23
	Feet frontal distance	10^{-4} 0.02	10^{-3} 0.31	10^{-5} 10^{-3}	0.01 0.07	10^{-4} 0.02	0.53 0.60

TABLE IV: Sobol indices for all six ergonomic indicators identified as relevant, for the drilling activity. For each parameter and indicator, the upper value is the first order index, the lower value is the total index. The ergonomic indicators are presented in decreasing order of importance (decreasing variance) from left to right: the percentages below their names correspond to the percentage of the total variance they explain. FTR stands for force transmission ratio. Numbers are colored from blue (minimum) to red (maximum), to facilitate the reading.

Parameter	Optim.	Init.
reference position for elbow flexion ($^{\circ}$)	135	100
drill handle orientation in slab plane / vertical ($^{\circ}$)	0	0
stab center height / shoulder height (m)	-0.1	0
offset distance pelvis - center of stab (m)	0.1	0
angle pelvis - normal to stab ($^{\circ}$)	-15	0
inter-feet distance in frontal plane (% of hip width)	200	120
inter-feet distance in sagittal plane (m)	-0.1	0

TABLE V: Optimal and initial parameters values for the drilling activity. The parameters which have the largest effect on performances enhancement are displayed in bold.

to conduct¹⁴. The initial gesture is also evaluated through an autonomous simulation, instead of through the replay of motion capture data, so that both situations are comparable. One of the five human subject is chosen as the reference for the initial situation (despite slight differences, all five subjects perform the gesture in a quite consistent way), in order to measure the values of the input parameters that must be used in the simulation. These values are displayed in table V, and the corresponding situations are illustrated in Fig. 7.

Table VI displays the values of the relevant indicators in both situations. Out of the six relevant indicators, five are significantly improved by the proposed modifications, whereas one - the back torque indicator - is slightly worsened. This might be due to the pelvis orientation (not facing the stab), which leads to increased torsion effort in the back.

In order to illustrate the reduced physical demands on more detailed biomechanical quantities, the evolution of the shoulder flexion and rotation torques during the whole drilling activity are plotted in Fig. 8, for the two situations. The shoulder joint is chosen as an example, because it is particularly

¹⁴A complete validation would however require the recording and replay of the gesture performed by a human subject following the recommendations.

	RA torque	Legs position	RA position	Back torque	FTR drilling	Balance margin
Init.	138	69	126	76	128	106
Modif.	98	40	108	83	107	69

TABLE VI: Values of the relevant ergonomic indicators in the initial and modified situation. RA stands for *right arm* and FTR for *Force Transmission Ratio*. For each indicator, the value displayed is the percentage of the indicator reference value (used for the scaling), so that the comparison is more understandable (the reference value gives an insight of the average order of magnitude of the indicator, however it does not provide any indication of the absolute level of risk).

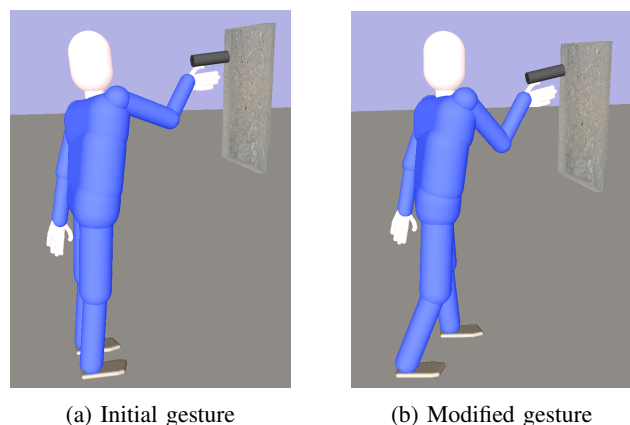


Fig. 7: Snapshots of the initial and modified drilling gesture simulated with the autonomous manikin.

used in the drilling activity, given both the drill weight to support and the drilling force to exert. Both joint torques are reduced during the modified gesture, and the simulation with the virtual manikin allows a quantitative estimation of

this reduction. The flexion torque decreases mainly because the increased elbow flexion reduces the moment associated with the drill weight (smaller lever arm). The rotation torque decreases mainly because the change in pelvis orientation (relative to the stab) modifies the transmission of the drilling force.

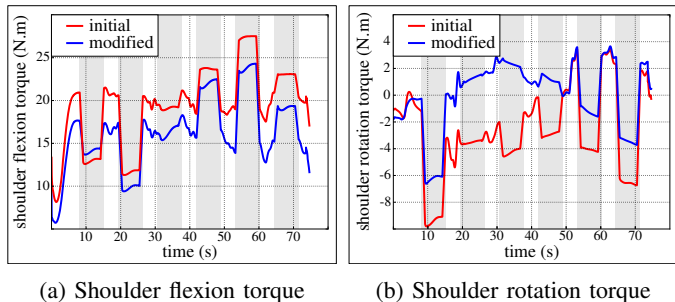


Fig. 8: Time evolution of the shoulder flexion and rotation torques in the initial and modified situations. The gray areas correspond to the drilling periods.

VI. DISCUSSION

The physically consistent results, as well as the enhanced performances obtained by following the recommendations provided through the proposed analysis demonstrate the usefulness of the method presented in this paper. However its application for the improvement of human gestures should be considered carefully because of some current limitations related to the human model and control, which are discussed thereafter.

A. Musculoskeletal model and motor control

Contrarily to the muscular actuation of the human body, the actuation of the manikin used in this work is only described at joint level (joint torques), and each joint is controlled by a unique actuator (1 per DoF). The biomechanical quantities measured with such a model are therefore less detailed than what could be achieved with a musculoskeletal model. For instance, the manikin joint torques do not fully represent the overall physical effort exerted by a person. Due to the redundancy of the human actuation, different combinations of muscle forces can result in a same joint torque. Internal muscle forces (*i.e.* forces which do not generate any joint torques) can thus be generated by a person, but they do not have any equivalent in the manikin model, and are therefore not accounted for in the evaluation. Such forces occur during the simultaneous contraction of antagonistic muscles (co-contraction phenomenon) and aim at increasing the joint impedance to withstand perturbations arising from limb dynamics or due to external loads [42]. Though especially important in motions requiring high accuracy, co-contraction occurs in all motions, in order to stabilize the joint, thus protecting joint structures. Not taking such forces into account therefore leads to a general under-estimation of the real human effort.

Nevertheless, the motion replay method presented in this work decouples the rigid body dynamics from the

actuation dynamics. The output of the dynamic replay fully describes the evolution of the system dynamics in terms of state $[\mathbf{q}^T(t), \dot{\mathbf{q}}^T(t)]^T$, joint torques $\boldsymbol{\tau}(t)$ and applied external wrenches $\mathbf{w}_c(t)$. Given this evolution, the use of an inverse musculoskeletal model (MM) could give access to the evolution of muscle activations $\mathbf{u}_m(t) = \mathbf{f}^{-1}(\mathbf{q}(t), \dot{\mathbf{q}}(t), \boldsymbol{\tau}(t), \mathbf{w}_c(t), MM)$. Muscle-related performance indicators could thus be estimated. In that sense, the proposed motion replay method is modular.

However, while replaying a motion does not require a model of whole-body motor control, such a model is needed for automatic motion generation. Indeed, simulating highly realistic human motions requires to account for the redundancy of the human musculoskeletal model as well as for the slow dynamics of human muscles activation. The slow dynamics is particularly limiting as it requires to consider the motor control problem from an optimal control point of view, rather than from a purely reactive one. The first consequence is a large increase in the computational cost, which is not compatible with running thousands of simulations in a reasonable amount of time (for the sensitivity analysis). Moreover, solving such an optimal control problem requires to understand the psychophysical principles that voluntary movements obey. Many studies have been conducted in order to establish mathematical formulae of such principles, especially for reaching motions (Fitt's law [43], minimum jerk principle [44], two-thirds power law [45]...). De Magistris *et al.* [46] have successfully applied some of them to virtual human simulations. However these improvements are currently limited to reaching motions, since driving principles are not yet known for all kinds of whole-body motions, especially when significant external forces are at play. Transposed to the manikin, determining the underlying principles of human motion comes down to establishing which mathematical quantities are minimized when human-like motions are performed. The determination of such optimality criteria can be investigated through inverse optimization techniques, as proposed by Clever *et al.* [47] for human locomotion, or by Berret *et al.* [48] for reaching motions, but it remains an open research problem.

B. Contacts placement

Since the sensitivity analysis is based on virtual human simulations, the biomechanical reliability of the results strongly depends on the realism of the autonomous manikin motion. Though the dynamic consistency of the motion is guaranteed, and most results presented in section V seem logical, it is not sufficient to prove the human-like behavior of the manikin. The realism of the manikin motion is especially significantly limited by its lack of autonomy regarding feet - as well as other possible contacts - placement. Indeed, the manikin feet positions are entirely set by the user and are therefore not necessarily well-adapted to the task (the manikin can walk or step, but the stepping time and destination must be specified beforehand).

In [49], Ibanez *et al.* propose a method for online adaptation of feet placement, which determines whether a step should be triggered, with which foot, and where. Activities including

locomotion, as well as adaptation steps can thus be addressed, though in the latter case a delay may be observed in the stepping motion. Indeed, adaptation steps are triggered to maintain balance while following the hands motion (if the hand motion is the one specified), whereas human beings usually anticipate such displacements.

Moreover, the method of Ibanez *et al.* only partly addresses the problem of contacts placement. Indeed, it is based on the ZMP concept and therefore remains limited to coplanar contacts. On the contrary, numerous gestures require a significant postural engagement which is achieved through the use of non-coplanar contacts: the feet can be on different planes (*e.g.* walking up stairs) and/or the hands can be used (*e.g.* pushing heavy objects, climbing). The problem of optimal - possibly non-coplanar - contacts placement has been addressed by Liu *et al.* [50] in the context of manipulation tasks with significant external forces. However this method is limited to activities during which the contacts do not change, because it is computationally expensive and cannot be run online to modify contacts placement during the simulation. More generally, the anticipated (*i.e.* not purely reactive) optimal placement of contacts usually requires complex planning methods [51], which for now are too computationally expensive to be used in the current context.

Despite the current limitations in the manikin motion, it should be noted that if the results of the sensitivity analysis presented in this paper (*i.e.* the relevant indicators and influential parameters, and their relations) are affected by these limitations, the method in itself is independent from the manikin control. Thus in the near future an improved control law could be used to animate the autonomous manikin, while the analysis method remains the same.

VII. CONCLUSION

This paper presents a method for automatically enhancing the performances of human gestures, based on a sensitivity analysis of human motion through motion replay, and virtual human simulations. The proposed method includes two components: one for replaying pre-recorded motions, and the other for analyzing the influence of the gesture parameters on the performances. The replay of motion capture data is achieved with an LQP controller, which guarantees the dynamic consistency of the resulting motion and forces. The initial gesture is thus acquired and evaluated through measurements conducted on a virtual manikin, and serves as an input for the sensitivity analysis. The analysis is based on virtual human simulations to estimate the performance indicators, for varying values of the input parameters, without the need for much input data. A variance-based analysis is used to extract the most relevant indicators, and sensitivity indices are computed for quantifying the influence of the parameters on the performance. Recommendations for gesture improvement are thereby provided. The whole method is applied to a drilling activity. The reliability of the motion and forces obtained through the replay method is successfully validated on 5 subjects. The results of the sensitivity analysis are partly qualitatively expected. However, the experiment

also demonstrates that the proposed analysis highlights and, most importantly, ranks some non trivial phenomena. Such phenomena can be explained afterwards, but they cannot be quantified *a priori*. In the end, the increased performances of the gesture modified according to the recommendations provided by the sensitivity analysis - in comparison with the initial gesture - demonstrates the usefulness of the proposed method. The realism of the autonomous manikin motion is however questioned. As a consequence, future work should be directed towards the improvement of the autonomous manikin control, in order to achieve more realistic motions. Nevertheless, the proposed sensitivity analysis method is tied neither to a specific human model, nor to a specific whole-body controller. As such, the method remains valid, independently from the model and control that are used.

APPENDIX A

DEFINITION OF SOBOL INDICES

Given X_i , $1 \leq i \leq d$, d random and mutually independent inputs of a model (in this work: the parameters of the gesture), and Y the output of the model (an indicator of performance), the variance of Y is decomposed as follows:

$$\begin{aligned} \text{Var}[Y] = & \sum_{i=1}^d V_i(Y) + \sum_i \sum_{\substack{j \\ j>i}} V_{ij}(Y) \\ & + \sum_i \sum_{\substack{j \\ j>i}} \sum_{\substack{k \\ k>j}} V_{ijk}(Y) + \dots + V_{1\dots d}(Y) \end{aligned} \quad (5)$$

where:

$$\begin{aligned} V_i(Y) &= \text{Var}[\mathbb{E}(Y|X_i)], \\ V_{ij}(Y) &= \text{Var}[\mathbb{E}(Y|X_i X_j)] - V_i(Y) - V_j(Y), \\ V_{ijk}(Y) &= \text{Var}[\mathbb{E}(Y|X_i X_j X_k)] \\ &\quad - \text{Var}[\mathbb{E}(Y|X_i X_j)] - \text{Var}[\mathbb{E}(Y|X_i X_k)] \\ &\quad - \text{Var}[\mathbb{E}(Y|X_k X_j)] \\ &\quad - V_i(Y) - V_j(Y) - V_k(Y), \end{aligned} \quad (6)$$

and so on. Sobol indices are then defined by:

$$S_i = \frac{V_i(Y)}{\text{Var}[Y]}, \quad S_{ij} = \frac{V_{ij}(Y)}{\text{Var}[Y]}, \quad \dots \quad (7)$$

Each index is between 0 and 1, and the sum of all indices is equal to 1. S_i is a first order index which represents the sensitivity of the model to X_i alone. A high S_i means that X_i alone strongly affects the output. S_{ij} is a second order index which represents the sensitivity of the model to the interaction between X_i and X_j , and so on. In order to simplify the interpretation of these indices when the model has numerous inputs, total sensitivity indices are defined as [52]:

$$S_{T_i} = S_i + \sum_{\substack{j \\ j \neq i}} S_{ij} + \sum_{\substack{j \\ j \neq i}} \sum_{\substack{k \\ k \neq i \\ k > j}} S_{ijk} + \dots \quad (8)$$

S_{T_i} represents all the effects of X_i on the model, including all interactions with other inputs. A small S_{T_i} means that X_i has very little influence on the output, even through interactions.

ACKNOWLEDGMENT

This work was partially supported by the RTE company through the RTE/UPMC chair "Robotics Systems for field intervention in constrained environments", held by Vincent Padois.

REFERENCES

- [1] E. Schneider and X. Irastorza, *OSH in figures: Work-related musculoskeletal disorders in the EU - Facts and figures*, European Agency for Safety and Health at Work, 2010.
- [2] NRC, *Musculoskeletal Disorders and the Workplace: Low Back and Upper Extremities*. Institute of Medicine and National Research Council, National Academy Press, 2001.
- [3] D. Fortenbaugh, G. Fleisig, and J. Andrews, "Baseball pitching biomechanics in relation to injury risk and performance," *Sports Health: A Multidisciplinary Approach*, vol. 1, no. 4, pp. 314–320, 2009.
- [4] J. Steele, "Biomechanical factors affecting performance in netball - implications for improving performance and injury reduction," *Sports Medicine*, vol. 10, no. 2, pp. 88–102, 1990.
- [5] D. L. Sturnieks, T. F. Besier, P. M. Mills, T. R. Ackland, K. F. Maguire, G. W. Stachowiak, P. Podsiadlo, and D. G. Lloyd, "Knee joint biomechanics following arthroscopic partial meniscectomy," *Journal of Orthopaedic Research*, vol. 26, no. 8, pp. 1075–1080, 2008.
- [6] S. Delp, F. Anderson, A. Arnold, P. Loan, A. Habib, C. John, E. Guendelman, and D. Thelen, "Opensim: open-source software to create and analyze dynamic simulations of movement," *IEEE Transactions on Biomedical Engineering*, vol. 54, no. 11, pp. 1940–1950, 2007.
- [7] M. Damsgaard, J. Rasmussen, S. T. Christensen, E. Surma, and M. de Zee, "Analysis of musculoskeletal systems in the anybody modeling system," *Simulation Modelling Practice and Theory*, vol. 14, no. 8, pp. 1100–1111, 2006.
- [8] J. Hicks, T. Uchida, A. Seth, A. Rajagopal, and S. Delp, "Is my model good enough? best practices for verification and validation of musculoskeletal models and simulations of movement," *Journal of biomechanical engineering*, vol. 137, no. 2, 2015.
- [9] E. Demircan, "Robotics-based reconstruction and synthesis of human motion," Ph.D. dissertation, Stanford University, 2012.
- [10] D. Thelen, F. Anderson, and S. Delp, "Generating dynamic simulations of movement using computed muscle control," *Journal of biomechanics*, vol. 36, no. 3, pp. 321–328, 2003.
- [11] D. Chaffin, G. Andersson, and B. Martin, *Occupational biomechanics*, 4th ed. Wiley, 2006.
- [12] J. Lee and S. Shin, "A hierarchical approach to interactive motion editing for human-like figures," *Proceedings of the 26th annual conference on Computer graphics and interactive techniques*, pp. 39–48, 1999.
- [13] K. Grochow, S. Martin, A. Hertzmann, and Z. Popović, "Style-based inverse kinematics," *ACM Transactions on Graphics*, vol. 23, no. 3, pp. 522–531, 2004.
- [14] F. Multon, R. Kulpa, L. Hoyet, and T. Komura, "Interactive animation of virtual humans based on motion capture data," *Computer Animation and Virtual Worlds*, vol. 20, no. 5–6, pp. 491–500, 2009.
- [15] M. Da Silva, Y. Abe, and J. Popović, "Simulation of human motion data using short-horizon model-predictive control," *Computer Graphics Forum*, vol. 27, no. 2, pp. 371–380, 2008.
- [16] U. Muico, Y. Lee, J. Popović, and Z. Popović, "Contact-aware nonlinear control of dynamic characters," *ACM Transactions on Graphics*, vol. 28, no. 3, p. 81, 2009.
- [17] C. John and B. Dariush, "Dynamically consistent human movement prediction for interactive vehicle occupant package design," *Proceedings of the 3rd Digital Human Modeling Symposium*, 2014.
- [18] C. Ott, D. Lee, and Y. Nakamura, "Motion capture based human motion recognition and imitation by direct marker control," *Proceedings of the 8th IEEE-RAS International Conference on Humanoid Robots*, pp. 399–405, 2008.
- [19] E. Demircan, T. Besier, S. Menon, and O. Khatib, "Human motion reconstruction and synthesis of human skills," *Advances in Robot Kinematics: Motion in Man and Machine*, pp. 283–292, 2010.
- [20] O. Khatib, "A unified approach for motion and force control of robot manipulators: The operational space formulation," *IEEE Journal of Robotics and Automation*, vol. 3, no. 1, pp. 43–53, 1987.
- [21] L. Sentis and O. Khatib, "A whole-body control framework for humanoids operating in human environments," *Proceedings of the IEEE International Conference on Robotics and Automation*, pp. 2641–2648, 2006.
- [22] J. Salimi, V. Padois, and P. Bidaud, "Synthesis of complex humanoid whole-body behavior: a focus on sequencing and tasks transitions," *Proceedings of the IEEE International Conference on Robotics and Automation*, pp. 1283–1290, 2011.
- [23] A. Escande, N. Mansard, and P. Wieber, "Hierarchical quadratic programming: Fast online humanoid-robot motion generation," *The International Journal of Robotics Research*, 2014.
- [24] S. Kajita, F. Kanehiro, K. Kaneko, K. Fujiwara, K. Harada, K. Yokoi, and H. Hirukawa, "Biped walking pattern generation by using preview control of zero-moment point," *Proceedings of the IEEE International Conference on Robotics and Automation*, vol. 2, pp. 1620–1626, 2003.
- [25] A. Saltelli, K. Chan, and E. Scott, *Sensitivity analysis*. Wiley, 2000.
- [26] W. Hoeffding, "A class of statistics with asymptotically normal distribution," *The annals of mathematical statistics*, pp. 293–325, 1948.
- [27] I. Sobol, "Sensitivity estimates for non linear mathematical models," *Mathematical Modelling and Computational Experiments*, pp. 407–414, 1993.
- [28] A. Saltelli, S. Tarantola, and K. Chan, "A quantitative model-independent method for global sensitivity analysis of model output," *Technometrics*, vol. 41, no. 1, pp. 39–56, 1999.
- [29] K. Campbell, M. McKay, and B. Williams, "Sensitivity analysis when model outputs are functions," *Reliability Engineering & System Safety*, vol. 91, no. 10, pp. 1468–1472, 2006.
- [30] M. Lamboni, H. Monod, and D. Makowski, "Multivariate sensitivity analysis to measure global contribution of input factors in dynamic models," *Reliability Engineering & System Safety*, vol. 96, no. 4, pp. 450–459, 2011.
- [31] I. Jolliffe, *Principal component analysis*. Wiley Online Library, 2002.
- [32] X. Merlihot, J. Le Garrec, G. Saupin, and C. Andriot, "The xde mechanical kernel: Efficient and robust simulation of multibody dynamics with intermittent nonsmooth contacts," *Proceedings of the 2nd Joint International Conference on Multibody System Dynamics*, 2012.
- [33] G. David, "Ergonomic methods for assessing exposure to risk factors for work-related musculoskeletal disorders," *Occupational medicine*, vol. 55, no. 3, pp. 190–199, 2005.
- [34] P. Maurice, Y. Measson, V. Padois, and P. Bidaud, "Experimental assessment of the quality of ergonomic indicators for collaborative robotics computed using a digital human model," *Proceedings of the 3rd Digital Human Modeling Symposium*, 2014.
- [35] C. Pholsiri, "Task-based decision making and control of robotic manipulators," Ph.D. dissertation, The University of Texas at Austin, 2004.
- [36] Y. Xiang, J. S. Arora, S. Rahmatalla, T. Marler, R. Bhatt, and K. Abdel-Malek, "Human lifting simulation using a multi-objective optimization approach," *Multibody System Dynamics*, vol. 23, no. 4, pp. 431–451, 2010.
- [37] S. Chiu, "Control of redundant manipulators for task compatibility," *Proceedings of the IEEE International Conference on Robotics and Automation*, vol. 4, pp. 1718–1724, 1987.
- [38] T. Yoshikawa, "Dynamic manipulability of robot manipulators," *Proceedings of the IEEE International Conference on Robotics and Automation*, vol. 2, pp. 1033–1038, 1985.
- [39] P. Maurice, P. Schlehuber, V. Padois, Y. Measson, and P. Bidaud, "Automatic selection of ergonomic indicators for the design of collaborative robots: A virtual-human in the loop approach," *14th IEEE-RAS International Conference on Humanoid Robots*, pp. 801–808, 2014.
- [40] V. De Sapio, "Task-level strategies for constrained motion control and human motion synthesis," Ph.D. dissertation, Stanford University, 2007.
- [41] G. Box and N. Draper, *Empirical model-building and response surfaces*. John Wiley & Sons, 1987.
- [42] P. Gribble, L. Mullin, N. Cothros, and A. Mattar, "Role of cocontraction in arm movement accuracy," *Journal of Neurophysiology*, vol. 89, no. 5, pp. 2396–2405, 2003.
- [43] P. Fitts, "The information capacity of the human motor system in controlling the amplitude of movement," *Journal of experimental psychology*, vol. 47, no. 6, p. 381, 1954.
- [44] T. Flash and N. Hogan, "The coordination of arm movements: an experimentally confirmed mathematical model," *The journal of Neuroscience*, vol. 5, no. 7, pp. 1688–1703, 1985.
- [45] P. Viviani and T. Flash, "Minimum-jerk, two-thirds power law, and isochrony: converging approaches to movement planning," *Journal of Experimental Psychology: Human Perception and Performance*, vol. 21, no. 1, p. 32, 1995.
- [46] G. De Magistris, A. Micaelli, P. Evrard, C. Andriot, J. Savin, C. Gaudez, and J. Marsot, "Dynamic control of dhm for ergonomic assessments," *International Journal of Industrial Ergonomics*, vol. 43, no. 2, pp. 170–180, 2013.

- [47] D. Clever, K. Hatz, and K. Mombaur, "Studying dynamical principles of human locomotion using inverse optimal control," *Proceedings in Applied Mathematics and Mechanics*, vol. 14, no. 1, pp. 801–802, 2014.
- [48] B. Berret, E. Chiovetto, F. Nori, and T. Pozzo, "Evidence for composite cost functions in arm movement planning: an inverse optimal control approach," *PLoS Comput Biol*, vol. 7, no. 10, 2011.
- [49] A. Ibanez, P. Bidaud, and V. Padois, "Emergence of humanoid walking behaviors from mixed-integer model predictive control," *Proceedings of the IEEE/RSJ International Conference on Intelligent Robots and Systems*, 2014.
- [50] M. Liu, A. Micaelli, P. Evrard, and A. Escande, "Task-driven posture optimization for virtual characters," *Proceedings of the 11th ACM SIGGRAPH/Eurographics conference on Computer Animation*, pp. 155–164, 2012.
- [51] K. Bouyarmane and A. Kheddar, "Multi-contact stances planning for multiple agents," *IEEE International Conference on Robotics and Automation*, pp. 5246–5253, 2011.
- [52] T. Homma and A. Saltelli, "Importance measures in global sensitivity analysis of nonlinear models," *Reliability Engineering & System Safety*, vol. 52, no. 1, pp. 1–17, 1996.